Transverse-field components of the flux-line lattice in the anisotropic superconductor $YBa_2Cu_3O_{7-\delta}$

P. G. Kealey,[1,*] D. Charalambous,[1] E. M. Forgan,[1] S. L. Lee,[2] S. T. Johnson,[3] P. Schleger,[4] R. Cubitt,[4] D. McK. Paul,[5] C. M. Aegerter,[6] S. Tajima,[7] and A. Rykov[7]

[1]*School of Physics and Astronomy, University of Birmingham, Birmingham B15 2TT, United Kingdom*

[2]*School of Physics and Astronomy, University of St. Andrews, St. Andrews, Fife KY16 9SS, United Kingdom*

[3]*Laboratoire de Physique des Solides, Bâtiment 510, Universite Paris-sud, 91405 Orsay, France*

[4]*Institut Laue-Langevin, 38042 Grenoble Cedex, France*

[5]*Department of Physics, University of Warwick, Coventry CV4 7AL, United Kingdom*

[6]*Physik-Institut der Universität Zürich, CH-8057, Switzerland*

[7]*Superconductivity Research Laboratory, ISTEC, Tokyo 135, Japan*

(Received 25 April 2001; published 27 September 2001)

We report on detailed small-angle neutron scattering measurements with *polarization analysis* from the flux-line lattice in the anisotropic superconductor $YBa_2Cu_3O_{7-\delta}$. When the field was applied at an angle to the principal axes we have observed spin-flip neutron diffraction consistent with local transverse field components. From a detailed study of the angle dependence of the magnitude of the spin-flip neutron-scattered intensity we have found that the transverse-field components are larger than predicted by an anisotropic London model for reasonable mass anisotropy values. The transverse-field components are consistent with a reduced *c*-axis coherence length at low temperature.

DOI: 10.1103/PhysRevB.64.174501 PACS number(s): 74.72.Bk, 74.60.Ge, 61.12.Ex

It is well known that many properties of high-temperature superconductors (HTS's) are anisotropic due mainly to the CuO_2 planes. With a field greater than H_{c1} applied parallel to the *c* axis, the screening currents associated with the flux-line lattice (FLL) flow in the plane perpendicular to the applied field. In an ideal isotropic superconductor this would be true for all angles of the applied field relative to the crystal axes. When the field is rotated away from the *c* direction in an anisotropic superconductor, the situation is complicated due to the reduced kinetic energy if current flows in an easy direction. The predicted current plane is tilted away from perpendicular to the applied field and towards the basal plane.

The tilted current flow results in *local* transverse-field components as proposed by Dorer and Bömmel[1] and later considered for the general case with $H_{c1} \ll H \ll H_{c2}$ by Thiemann *et al.*[2] By a flux quantization argument,[3] one may show that the flux-line cores lie along the direction of the *average* magnetic field. Hence, there is a zero spatial average of the local fields transverse to the flux lines. These fields are distinct from any transverse magnetization[4] and can therefore only be detected by a microscopic probe. The variation of both the longitudinal and transverse fields in the FLL gives rise to small-angle neutron scattering (SANS), but the transverse fields also *flip* the spin of the diffracted neutrons. In this paper we present the first SANS measurements with *polarization analysis* from the mixed state of $YBa_2Cu_3O_{7-\delta}$ (YBCO). Our technique is quite different from neutron depolarization[5] which gives a measure of larger scale field gradients by the depolarization of the *transmitted* beam. Such effects were undetectably small in our experiments. We have observed spin-flip neutron diffraction consistent with the predicted transverse-field components and make a comparison between our experimental observations and the anisotropic London model which we now describe.

For a moderately anisotropic superconductor such as YBCO with large κ and a coherence length comparable with the interplane spacing, an appropriate theory is the anisotropic London model,[6] particularly close to T_c. This theory has the advantage that it provides a simple and successful description of the magnetic response of anisotropic superconductors. However, the model is phenomenological, as it does not include the underlying physical origin of the anisotropy.

In the anisotropic London model, the effective mass of the charge carriers depends on their direction of motion. The normalized effective masses are written as m_a, m_b, and m_c and are normalized to the "average mass" $M_{av} = (M_b M_a M_c)^{1/3}$ such that $m_i = M_i / M_{av}$ and $m_a m_b m_c = 1$. The anisotropy may be quantified as two ratios of the effective masses: $\gamma_{ca}^2 = m_c / m_a$ and $\gamma_{ab}^2 = m_a / m_b$. The supercurrent response is larger in the *b* direction than the *a* direction due to the Cu-O chains. The result is a shorter penetration depth λ_b for fields in the *c* direction which are varying along *a* than the corresponding penetration depth λ_a for fields varying along *b*. Hence the FLL is distorted. We have shown in previous SANS measurements on our sample under similar conditions to here that $\gamma_{ca} = 4.5(6)$ and $\gamma_{ab} = 1.18(2)$.[7]

We will now examine the predictions of an anisotropic model using the nomenclature of Thiemann *et al.*,[2] extending their analysis to the case of biaxial anisotropy, i.e., $m_a \neq m_b$. In the mixed state, the magnetic field distribution $\mathbf{B}(\mathbf{r})$ may be represented by the Fourier series

$$\mathbf{B}(\mathbf{r}) = \sum_{\mathbf{q}} \mathbf{b}(\mathbf{q}) \exp(i\mathbf{q}\cdot\mathbf{r}), \tag{1}$$

where $\mathbf{q}$ is the set of reciprocal lattice vectors.[8] The average field is in the *z* direction and the transverse fields $B_x(\mathbf{r})$ and $B_y(\mathbf{r})$ are in the *xy* plane, defined in Fig. 1. In an isotropic

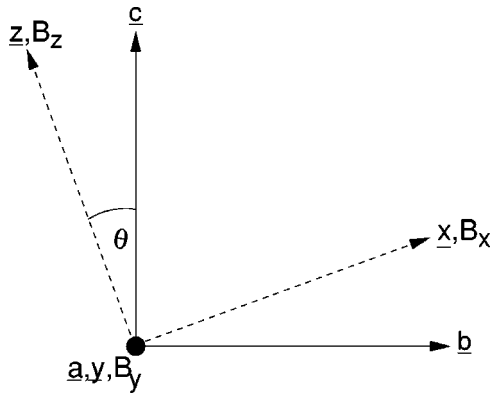

FIG. 1. Diagram of the coordinate system used in this paper. The crystal axes are represented by crystallographic labels *a*, *b*, and *c*. The coordinate system of the FLL is labeled *x*, *y*, and *z*. The *z* axis is parallel to the direction of the average field in the sample. In the experiment the field was always in the *b*-*c* plane, at an angle θ to the crystal *c* direction.

superconductor $b_x(\mathbf{q})=b_y(\mathbf{q})=0$; $b_z(\mathbf{q})\neq 0$, and the average field and the local field are parallel to the applied field. Extending the derivation of Eq. (7) of Ref. 2, but with the inclusion of *a*-*b* anisotropy, one obtains after straightforward algebra the components of the Fourier coefficient $\mathbf{b}(\mathbf{q})$:

$$b_x(\mathbf{q})=\lambda^2 m_{xz} q_y^2 B/d, \tag{2}$$

$$b_y(\mathbf{q})=-\lambda^2 m_{xz} q_x q_y B/d, \tag{3}$$

$$b_z(\mathbf{q})=B(1+\lambda^2 m_{zz} q^2)/d, \tag{4}$$

where

$$d=(1+\lambda^2 m_{yy} q_x^2+\lambda^2 m_{xx} q_y^2)(1+\lambda^2 m_{zz} q^2)-\lambda^4 m_{xz}^2 q^2 q_y^2, \tag{5}$$

and B is the average field, λ is the value that the London penetration depth would have for the average mass M_{av}, and θ, *x*, *y*, and *z* are defined in Fig. 1. The masses m_{ij} are the components of the rotated effective mass tensor

$$\mathbf{M}=\begin{pmatrix} m_{xx} & 0 & m_{xz} \\ 0 & m_a & 0 \\ m_{xz} & 0 & m_{zz} \end{pmatrix}, \tag{6}$$

where $m_{xx}=m_b\cos^2\theta+m_c\sin^2\theta$, $m_{xz}=(m_b-m_c)\sin\theta\cos\theta$ and $m_{zz}=m_b\sin^2\theta+m_c\cos^2\theta$.[2]

From Eqs. (2) and (3) it may be seen that when the average field is at an angle to the principal axes ($\theta\neq 0$) there exist transverse field components $b_x(\mathbf{q})$ and $b_y(\mathbf{q})$ as $m_b \neq m_c$.

The measurements were performed on a large (1.072 g) untwinned single-crystal $YBa_2Cu_3O_{7-\delta}$ sample used in previous SANS measurements.[7] From characterization measurements the sample is known to be essentially single domain[9] which allows discrimination between the crystallographic *a* and *b* directions and therefore determination of γ_{ab}. The experiments were performed on the IN15 spectrometer at the Institut Laue Langevin with 10-Å cold neutrons.[10] The

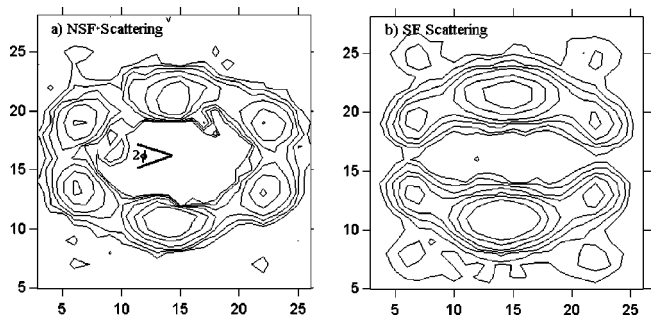

FIG. 2. Contour plots of (a) the non-spin-flip and (b) the spin-flip neutron diffraction patterns from the FLL of $YBa_2Cu_3O_{7-\delta}$. Data are the sum of that obtained by rocking about a vertical axis the sample through the Bragg scattering condition for the left and right spots. This sum shows the symmetry of the FLL but tends to broaden the image of the top and bottom spots which are never exactly on the Bragg condition. A field of 0.5 T was applied in the *b*-*c* plane at 60° to the *c* axis. The diffracted signal was obtained by subtracting data taken above T_c. The axes represent pixel numbers and the center of the detector has been masked. The scattering vectors q_x and q_y are defined as horizontal and vertical, respectively. The angle 2ϕ is a measure of the distortion of the FLL.

sample was mounted with the *a* axis vertical between the coils of a split-pair cryomagnet with the ability to rotate the crystal and apply the field at an arbitrary angle in the horizontal *b*-*c* plane.

The spectrometer receives a longitudinally polarized neutron beam traveling approximately parallel to the field in the sample. In our setup the neutron polarization was maintained by longitudinal fields provided by solenoids before and after the sample. By operating a spin flipper, the incident polarization could be changed from parallel to antiparallel to the field. The transmitted and scattered neutrons passed through a second flipper, then a set of analyzer supermirrors in front of a 32×32 cm^2 multidetector. The analyzers are arranged to absorb the incident neutron polarization; thus spin-flipped neutrons would mainly be detected with neither or both flippers operating and non spin flipped when one flipper was operating. The beam polarization and the pixel-by-pixel flipper and analyzer efficiencies were calibrated by placing the non-spin-flip scatterer pyrolitic graphite in the beam and by counting with all four possible flipper combinations. Further details of IN15 in SANS mode with *polarization analysis* are detailed elsewhere.[11] The FLL was established in the sample by cooling in the applied field of 0.5 T. The magnetization of the sample was negligible and the average direction of the flux lines trapped in the sample was within 0.25° of the applied field.

We have measured the non-spin-flip (NSF) and spin-flip (SF) diffraction for a field of 0.5 T applied at nine angles between 0 and 80° to the *c* axis in the *b*-*c* plane. For each field orientation, the crystal and field were rocked together through the FLL Bragg scattering condition and background data taken at 100 K was subtracted from the foreground taken at 2 K after field cooling. In each case, data were taken for all four flipper combinations and, using our calibrations, converted to SF and NSF scattering intensities. In Fig. 2(a) is shown the NSF diffraction signal with the field applied at

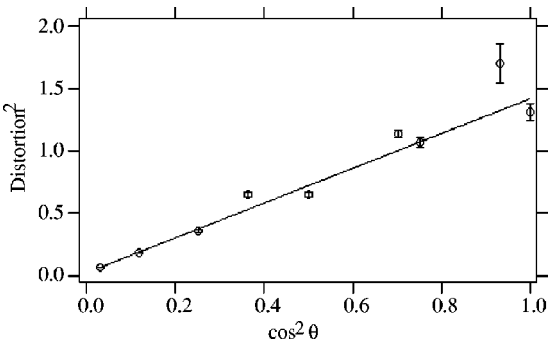

FIG. 3. Distortion of the FLL as a function of the angle of the applied magnetic field from the *c* axis. The distortion was deduced by fitting the spots on the detector and determining the angle between the scattering vectors as detailed in Eq. (7).

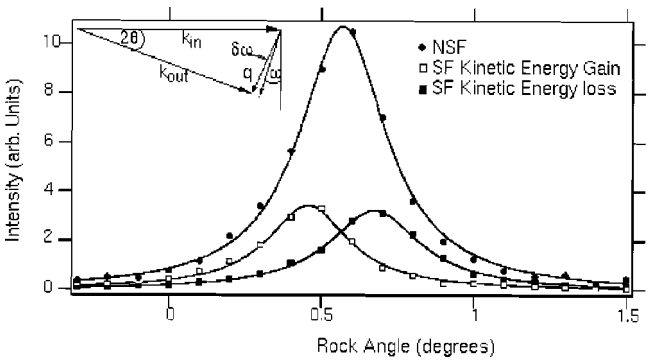

FIG. 4. Rocking angle dependence of the scattered neutron intensity from the FLL for a field of 0.5 T applied in the *b*-*c* plane at an angle of 60° to the *c* axis. The intensity for the non-spin-flip and the spin-flip scattering is plotted. Two initial spin directions are plotted for the case of spin-flip scattering, corresponding to kinetic energy gain and loss. The observed splitting $\delta\omega$ in the peak intensity ω angle is due to the Zeeman splitting of the neutron potential energy in the sample region which means $k_{\rm in} \neq k_{\rm out}$ as shown in the inset.

60° to the *c* axis. The crystal anisotropy results in the spots forming a distorted hexagon. It has been shown that the distortion of the FLL is given by[12]

$$\text{distortion}^2 = \left(\frac{\tan\phi}{\tan 30°}\right)^2 = \gamma_{ab}^2 \cos^2\theta + \frac{1}{\gamma_{ca}^2}\sin^2\theta, \qquad (7)$$

where 2ϕ is the angle between the first-order scattering vectors shown in Fig. 2(a). To determine the distortion, the diffraction spots were fitted to two-dimensional (2D) Gaussians and from their positions the angle ϕ could be calculated. The spot position was fitted at the rocking angle corresponding to the peak intensity. The distortion as a function of the angle of the applied field is plotted in Fig. 3. The distortion was fitted to Eq. (7) and from the fit parameters we deduce $\gamma_{ab} = 1.19(1)$ and $\gamma_{ca} = 6.0(4)$. From these values using Eqs. (2) and (3) we can calculate the magnitude of the transverse-field components and therefore the expected magnitude of the SF scattering in the anisotropic London model.

Other techniques may also be used to deduce the mass anisotropy: they include muon spin rotation (μSR),[13] torque magnetometry,[4,13,14] infrared reflectivity,[15] Josephson tunneling,[16] and Bitter decoration.[17] Using torque magnetometry and μSR, on the same sample as used in this SANS study, we have found $\gamma_{ab} = 1.15(1)$.[13] There is reasonable agreement on the value of γ_{ab} between a wide range of techniques on a number of different crystals: Bitter decoration, SANS, μSR, and torque give a value of $\gamma_{ab} = 1.1 \rightarrow 1.2$. However, Josephson tunneling and IR reflectivity lead to values in the range $\gamma_{ab} = 1.2 \rightarrow 1.7$ which may be due to variations in the perfection of the Cu-O chains. There is much less agreement between different techniques for the out of plane anisotropy γ_{ca},[13] which may be understood in part as γ_{ca} depends on oxygen content.[18] On the same crystal as used in this study we have found, by μSR at 50 K, $\gamma_{ca} = 3.7(5)$, whereas torque magnetometry at 93 K is consistent with $\gamma_{ca} = 6.6(5)$.

In Fig. 2(b) we present the SF diffraction pattern. The diffraction spots show the same long-range periodic structure of the FLL as seen in Fig. 2(a), which is evidence that the origin of this signal is SF diffraction from transverse fields in the FLL. With the field applied parallel to the *c* axis we observe, within errors, zero spin-flip scattering. It is interesting to note that the SF scattering may actually be seen in the unsubtracted data as there is very little background SF scattering from defects or other sources.

Before presenting a study of the angle dependence of the SF scattering, we will examine some details of the spin-flip diffraction pattern. In Fig. 2(b) it can be seen that for $q_y = 0$ there is zero SF scattering. This is expected from Eqs. (2) and (3) as both $b_x(\mathbf{q})$ and $b_y(\mathbf{q})$ are zero for $\mathbf{q} = (q_x, 0)$. The b_x result arises from the Maxwell equation div $\mathbf{B}(\mathbf{r}) = 0$, which may be expressed in reciprocal space as $\mathbf{q} \cdot \mathbf{b}(\mathbf{q}) = 0$. From mirror symmetry of the FLL about $y = 0$ $b_y(q_x, 0)$ is also zero, so there should be no SF scattering for $q_y = 0$.

When the neutron spin is flipped in a magnetic field there is a change in the potential energy of the neutron equal to the Zeeman splitting for the neutron. From conservation of energy, this results in a change of the neutron kinetic energy. Although small (≈ 60 neV) this noticeably changes the angle ω through which the sample must be rotated to bring the scattering vector to a reciprocal lattice point. The change is given by $\delta\omega/\omega = \pm 1.91/2\pi$ and is positive for a decrease in kinetic energy. In Fig. 4 we plot the intensity of the NSF and SF scattering as a function of the rocking angle ω. By changing the incident neutron polarization, SF scattering with either kinetic energy gain or loss was probed. The observed splitting is consistent with the predicted value of $\pm 0.15°$ for an applied field of 0.5 T.

We now examine the angular dependence of the SF and NSF scattering for the four spots near the horizontal plane (we ignore the vertical spots because we did not have the facility to rock through the Bragg condition for them). A reliable measure of the intensity of the spin-flip diffraction is the ratio of the integrated SF and NSF intensities. This ratio is independent of many possible systematic experimental errors. The quantization axis for the neutron spin is the average magnetic field direction *z*. Just as in NMR, varying perpen-

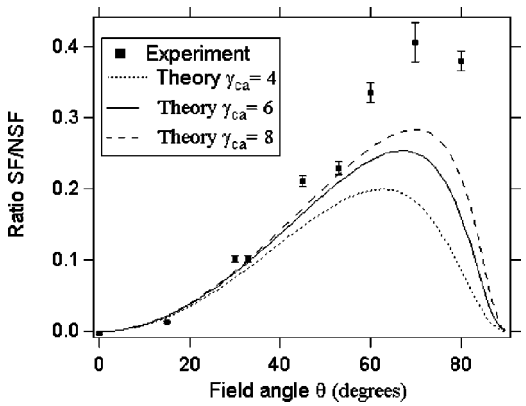

FIG. 5. Plot of the ratio of the theoretical and experimental SF to NSF scattering as a function of the applied field direction. The experimental intensities were evaluated as the sum of the counts in a small area of the detector centerd on the NSF spot position, integrated over the rocking curve. The theoretical plots are calculated using $\gamma_{ab}=1.19$ and for $\gamma_{ca}=4$, 6, and 8.

dicular magnetic fields flip the neutron spin, so that the integrated SF intensity is proportional to $b_x^2+b_y^2$.[19] Fields varying parallel to the quantization axis cannot cause transitions, so the integrated NSF intensity is proportional to b_z^2. The ratio r_{SF} of the SF and NSF integrated intensities is therefore given by

$$r_{SF}=\frac{b_x^2+b_y^2}{b_z^2}=\frac{m_{xz}^2(q_y^4+q_x^2q_y^2)}{m_{zz}^2q^4}, \tag{8}$$

which may easily be evaluated as a function of θ and the anisotropy parameters γ_{ab} and γ_{ca}. In Fig. 5 we plot the experimental ratio of the SF and NSF integrated intensities and compare with the prediction of Eq. (8). The theoretical lines in Fig. 5 are plotted for a range of γ_{ca} values predicted from various techniques[13–17] as well as that deduced from the FLL distortion. The experimental ratio is greater than that predicted by the anisotropic London theory for any reasonable values of γ_{ab} and γ_{ca}.

It should be noted that *distortion* of the FLL is governed by the high-temperature mass anisotropy, at the point where the FLL becomes pinned. However, the transverse-field components will be governed by the low-temperature anisotropy. The data could be fitted by the anisotropic London model with a much larger out of plane anisotropy ($\gamma_{ca}\sim 50$), which would correspond to a much greater confinement of supercurrent flow to the Cu-O planes as the *c*-axis coherence length ξ_c becomes much smaller than the interplanar spacing. However, under such conditions the layered crystal structure becomes important and a continuum London theory should not apply. Nonlocal effects[20,21] can also give deviations from the London model, although it is not clear that they would result in an increased anisotropy γ_{ca} in YBCO. In any case, we conclude that the anisotropic London model does not give an accurate description of $YBa_2Cu_3O_{7-\delta}$ at low temperature where the superconductivity appears more two dimensional than at high temperatures. It would be of interest to study this over a range of temperatures.

We acknowledge the technical expertise of G. R. Walsh in the design and construction of the cryomagnet used in these SANS experiments. This work was supported by the U.K. E.P.S.R.C., NEDO Japan for the R&D of Industrial Science and Technology Frontier Program, and the neutron scattering was carried out at the Institut Laue-Langevin, Grenoble.

*Electronic address: P.G.Kealey@bham.ac.uk

[1] G.L. Dorer and H.E. Bömmel, Phys. Rev. **183**, 528 (1969).
[2] S.L. Thiemann, Z. Radovic, and V.G. Kogan, Phys. Rev. B **39**, 11 406 (1989).
[3] V.G. Kogan and J.R. Clem, Phys. Rev. B **24**, 2497 (1981).
[4] D.E. Farrell, C.M. Williams, S.A. Wolf, N.P. Bansal, and V.G. Kogan, Phys. Rev. Lett. **61**, 2805 (1988).
[5] W. Roest and M. Th. Rekveldt, Phys. Rev. B **48**, 6420 (1993).
[6] V.G. Kogan, Phys. Rev. B **24**, 1572 (1981).
[7] S.T. Johnson, E.M. Forgan, S.H. Lloyd, C.M. Aegerter, S.L. Lee, R. Cubitt, P.G. Kealey, C. Ager, S. Tajima, A. Rykov, and D.McK. Paul, Phys. Rev. Lett. **82**, 2792 (1999).
[8] P.G. Kealey, T.M. Riseman, E.M. Forgan, L.M. Galvin, A.P. Mackenzie, S.L. Lee, D.McK. Paul, R. Cubitt, D.F. Agterberg, R. Heeb, Z.Q. Mao, and Y. Maeno, Phys. Rev. Lett. **84**, 6094 (2000).
[9] E. M. Forgan, P. G. Kealey, and A. Rykov (unpublished).
[10] P. Schleger, G. Ehlers, A. Kollmar, B. Alefeld, J.F. Barthelemy, H. Casalta, B. Farago, P. Giraud, C. Hayes, C. Lartigue, F. Mezei, and D. Richter, Physica B **266**, 49 (1999).
[11] E.M. Forgan, P.G. Kealey, T.M. Riseman, S.L. Lee, D.McK. Paul, C.M. Aegerter, R. Cubitt, P. Schleger, A. Pautrat, C. Simon, and S.T. Johnson, Physica B **267-268**, 115 (1999).
[12] M. Yethiraj, H.A. Mook, G.D. Wignall, R. Cubitt, E.M. Forgan, S.L. Lee, D.McK. Paul, and T. Armstrong, Phys. Rev. Lett. **71**, 3019 (1993).
[13] C. Ager, F.Y. Ogrin, S.L. Lee, C.M. Aegerter, S. Romer, H. Keller, I.M. Savic, S.H. Lloyd, S.T. Johnson, E.M. Forgan, T.M. Riseman, and P.G. Kealey, Phys. Rev. B **62**, 3528 (2000).
[14] T. Ishida, K. Okuda, H. Asaoka, Y. Kazumata, K. Noda, and H. Takei, Phys. Rev. B **56**, 11 897 (1997).
[15] D.N. Basov, R. Liang, D.A. Bonn, W.N. Hardy, B. Dabrowski, M. Quijada, D.B. Tanner, J.P. Rice, D.M. Ginsberg, and T. Timusk, Phys. Rev. Lett. **74**, 598 (1995).
[16] A.G. Sun, S.H. Han, A.S. Katz, D.A. Gajewski, M.B. Maple, and R.C. Dynes, Phys. Rev. B **52**, 15 731 (1995).
[17] G.J. Dolan, F. Holtzberg, C. Feild, and T.R. Dinger, Phys. Rev. Lett. **62**, 2184 (1989).
[18] S. Kokkaliaris, K. Deligiannis, M. Oussena, A.A. Zhukov, P.A.J. de Groot, R. Gagnon, and L. Taillefer, Supercond. Sci. Technol. **12**, 690 (1999).
[19] N.K. Zhuchenko, Physica C **206**, 133 (1993).
[20] Y. De Wilde, M. Iavarone, U. Welp, V. Metlushko, A.E. Koshelev, I. Aranson, G.W. Crabtree, and P.C. Canfield, Phys. Rev. Lett. **78**, 4273 (1997).
[21] M.H.S. Amin, M. Franz, and I. Affleck, Phys. Rev. Lett. **84**, 5864 (2000).